Vegetation and Induration as Sand Dunes Stabilizators

Article *in* Journal of Coastal Research · November 2008

DOI: 10.2112/08A-0011.1

CITATIONS
40

READS
752

4 authors, including:

Orencio Durán
MARUM Center for Marine Environmental Sciences
70 PUBLICATIONS **3,196** CITATIONS

SEE PROFILE

Eric Parteli
University of Duisburg-Essen
110 PUBLICATIONS **3,753** CITATIONS

SEE PROFILE

Vegetation and induration as sand dunes stabilizators.

Hans J. Herrmann[1,2], Orencio Durán[1], Eric J. R. Parteli[1] and Volker Schatz[1].
1. Institut für Computerphysik, ICP, Pfaffenwaldring 27, 70569 Stuttgart, Germany.
2. Departamento de Física, Universidade Federal do Ceará, 60455-970, Fortaleza, CE, Brazil.

September 22, 2006

Sand dunes are found in a wide variety of shapes in deserts and coasts, and also on the planet Mars. The basic mechanisms of dune formation could be incorporated into a continuum saltation model, which successfully reproduced the shape of the barchan dunes and has been also applied to calculate interaction of barchans in a field. We have recently extended our dune model to investigate other dune shapes observed in nature. Here, we present the first numerical simulation of the transformation of barchan dunes, under influence of vegetation, into parabolic dunes, which appear frequently on coasts. Further, we apply our model to reproduce the shape of barchan dunes observed on Mars, and we find that an interesting property related to the martian saltation is relevant to predict the scale of dunes on Mars. Our model could also reproduce unusual dune shapes of the Martian north polar region, like rounded barchans and elongated linear dunes. Our results support the hypothesis that these dunes are indurated.

1 Introduction

Sand dunes develop wherever sand is exposed to an agitated medium that lifts grains from the ground and entrains them into a surface flow. On coasts, dunes are constituted of sand which comes from the sea and is therafter deposited onto the beach. Once the grains are exposed to the air, they dry and some can be carried by the wind, initiating sand transport.

The morphology of sand dunes and the conditions under which each dune type appears in coastal areas have been studied by several authors. Quantitatively, however, the selection of dune size and shape and the mechanisms of coastal dunes stabilization are far from being understood, and are the challenges which motivate the present work.

The mechanism responsible for dune formation is called *saltation* (Bagnold 1941; Owen 1964; White 1979; Ungar and Haff 1987; Anderson and Haff 1991; McEwan and Willetts 1991; Rasmussen et al. 1996; Foucaut and Stanilas 1997; Dong et al. 2005; Almeida et al. 2006). Grains are lifted from the ground by the wind, accelerated downwind, and after a certain distance ℓ they collide back onto the ground. Each impact grain may eject further grains — a mechanism called "splash" (Anderson and Haff 1988; Nalpanis et al. 1993) — and thus a cascade process occurs, until the saltation flux achieves saturation, since the air transfers momentum back to the grains. Dunes appear because an exposed sand sheet is unstable, evolves into hills, and next into dunes with a slip face. The existence of a saturation transient of the sand flux is reponsible for the existence of a minimum dune size.

1.1 The Dune Model

We have recently proposed a minimal dune model which provides an understanding of important features of real dunes, such as their longitudinal shape and aspect ratio, the formation of a slip face, the breaking of scale invariance, and the existence of a minimum dune size (Sauermann et al. 2001; Kroy et al. 2002). This model combines an analytical description of the turbulent wind velocity field above the dune with a continuum saltation model that allows for saturation transients in the sand flux. The fundamental idea of the dune model is to consider the bed-load as a thin fluid-like granular layer on top of an immobile sand bed. The model has been latter improved by Schwämmle and Herrmann (2005) to take into ac-

count lateral sand transport due to perturbations transverse to the main wind direction.

In previous works we studied the formation and evolution of barchans and transverse dunes. In particular we could successfully reproduce the crescent shape of dunes which develop in areas of unidirectional winds, their rate of motion, stability and interaction with each other. There are, indeed, several different sand patterns which can be observed on coasts according to wind condition, sand availability, humidity level and vegetation. A model of sand dunes which accounts for such variables yields an advantageous tool in the understanding of coastal processes and morphology.

Here we present some new results we obtained from an extension of our model to study dunes with vegetation, which are ubiquitous on coasts. Furthermore, we investigate the significance of sand induration for the morphology of rounded barchans in the north polar region of Mars, which resemble the oil-soaked terrestrial dunes of Kerr and Nigra (1952). Our calculations of Mars dunes provide a new insight into the modelling of the saturation length, and are therefore of fundamental importance to understand the formation of coastal sand dunes, their characteristic size and shape. In this section, a summary of the main ingredients of the dune model is presented.

1.1.1 Wind shear stress

Sand transport takes place near the surface, in the turbulent boundary layer of the atmosphere (Pye and Tsoar 1991). In this turbulent layer, the wind velocity $u(z)$ at a height z may be written as

$$u(z) = \frac{u_*}{\kappa} \ln \frac{z}{z_0}, \tag{1}$$

where $\kappa = 0.4$ is the von Kármán constant, u_* is the wind shear velocity, which is used to define, together with the fluid density ρ_{fluid}, the shear stress $\tau = \rho_{\text{fluid}} u_*^2$, and z_0 is called aerodynamic roughness.

A dune or a smooth hill can be considered as a perturbation of the surface that causes a perturbation of the air flow onto the hill. In the model, the shear stress perturbation is calculated in the two dimensional Fourier space using the algorithm of Weng et al. (1991) for the components τ_x and τ_y, which are, respectively, the components parallel and perpendicular to wind direction. In what follows, we present the sand transport equations introduced in Sauermann et al. (2001) and refer to Schwämmle and Herrmann (2005) for a two-dimensional extension of the model.

1.1.2 Continuum saltation model for sand transport

The sand transport model uses the air shear stress in the boundary layer to calculate the sand flux. The equation for the sand flux (Sauermann et al. 2001) is a differential equation that contains the saturated flux q_{s} at the steady state, and the characteristic length ℓ_{s} that defines the transients of the flux:

$$\frac{\partial}{\partial x} q = \frac{1}{\ell_{\text{s}}} q \left(1 - \frac{q}{q_{\text{s}}} \right). \tag{2}$$

In eq. (2), the saturation length ℓ_{s} is written as

$$\ell_{\text{s}} = \frac{1}{\gamma} \left[\frac{\ell}{\left(u_* / u_{*\text{t}} \right)^2 - 1} \right], \tag{3}$$

where ℓ is the average saltation length and $u_{*\text{t}}$ is the threshold wind shear velocity for sustained saltation, which defines the threshold shear stress $\tau_{\text{t}} = \rho_{\text{fluid}} u_{*\text{t}}^2$. The parameter γ models the average number n of grains dislodged out of equilibrium, and is written as

$$\gamma = \frac{\mathrm{d}n}{\mathrm{d}(\tau_{\text{a}}/\tau_{\text{t}})}, \tag{4}$$

where τ_{a} is the air born shear stress, which is distinguished from the grain born shear stress, i.e. the contribution of the saltating grains near the ground to the total shear stress τ due to their impacts onto the surface. The parameter γ, thus, gives the amount of grains launched into the saltation sheet when the wind strength deviates from the threshold by an amount $\tau_{\text{a}}/\tau_{\text{t}}$. The air born shear stress τ_{a} is lowered if the number of grains in the saltation layer increases and vice versa, which is called the "feedback" effect: At threshold, the wind has a strength $\tau_{\text{a}} \approx \tau_{\text{t}}$ sufficient to just maintain saltation. The parameter γ depends on microscopic quantities such as the time of a saltation trajectory or the grain-bed interaction, which are not available in the scope of the model.

The steady state is assumed to be reached instantaneously, since it corresponds to a time scale several orders of magnitude smaller than the time scale of the surface evolution. Thus, time dependent terms are neglected.

1.1.3 Surface evolution

The time evolution of the topography $h(x,t)$ is given by the mass conservation equation

$$\frac{\partial h}{\partial t} = -\frac{1}{\rho_{\text{sand}}} \frac{\partial q}{\partial x}, \tag{5}$$

where $\rho_{\text{sand}} = 0.62\rho_{\text{grain}}$ is the mean density of the immobile dune sand (Sauermann et al. 2001), while ρ_{grain} is the grain density. If sand deposition leads to slopes that locally exceed the angle of repose $\theta_{\text{r}} \approx 34^\circ$ of the sand, the unstable surface relaxes through avalanches in the direction of the steepest descent. Avalanches are assumed to be instantaneous since their time scale is negligible in comparison with the time scale of the dunes.

For a dune with slip face, flow separation occurs at the brink, which represents a discontinuity of the surface. The flow is divided into two parts by streamlines connecting the brink with the ground. These streamlines define the separation bubble, inside which eddies occur and the flow is often re-circulating (Kroy et al. 2002). In the model, the dune is divided into several slices parallel to wind direction, and for each slice, one separation streamline is defined at the lee side of the dune. Each streamline is fitted by a third order polynomial connecting the brink with the ground, at the reattachment point. The distance between the brink and the reattachment point, and thus the length of the separation bubble is determined by the constraint of a maximum slope of 14° for the streamlines (Kroy et al. 2002). Inside the separation bubble, the wind shear stress and sand flux are set to zero.

Simulation steps may be summarized as follows: (i) the shear stress over the surface is calculated using the algorithm of Weng et al. (1991); (ii) from the shear stress, the sand flux is calculated with eq. (2); (iii) the change in the surface height is computed from mass conservation (eq. (5)) using the calculated sand flux; and (iv) if the inclination of the surface gets larger than θ_{r}, avalanches occur and a slip face is developed. Steps (i) $-$ (iv) are iteratively computed until the steady state is reached.

1.2 Barchan dunes and barchan fields

In spite of its apparent complexity, the procedure presented above is so far the simplest method for calculating the evolution of sand dunes. In particular for barchan dunes the dune model has been extensively tested and its results have been found to be quantitatively in good agreement with field measurements (Sauermann et al. 2003). Moreover, the model has been applied to calculate interaction of barchan dunes in a field, and revealed that dunes may interact in different ways, depending on their sizes. Since smaller dunes have higher velocities, they may easily "collide" with larger, slower wandering ones during their downwind motion in a field. Our simulations show that very small dunes in this case may be "swallowed up" by larger dunes downwind. But if the size difference between the interacting dunes is not too large, then the smaller dune upwind gains sand from the larger one, which then becomes smaller and may wander away (fig. 1). Effectively, it is like if the smaller dune were crossing over the larger one (Schwämmle and Herrmann 2003), as proposed recently by Besler (1997). A systematic study of dune interaction has been presented in Durán et al. (2005).

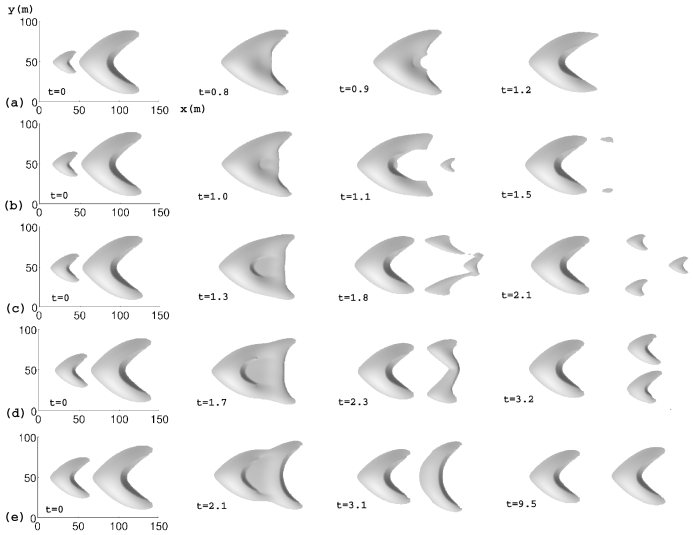

Figure 1. Four simulation snapshots of barchan dune interaction. Cases (a) — (e) correspond to different initial heights for the upwind, smaller barchan (Durán et al. 2005).

Many times, however, dunes meet obstacles and cannot evolve freely on bedrocks or sand sheets under the action of wind. A classical example is the case of most coastal dunes. Dunes wandering onto the continent often compete with vegetation, which grows close to the sea where it finds favorable, humid conditions. We all know that plants fix the sand on the ground, but we also expect that the efficiency to stop sand transport should depend for instance on vegetation amount. We investigated with our dune model what happens with a barchan dune when it encounters a vegetated area. Tsoar and Blumberg (2002) proposed that barchans should transform into parabolic dunes under the influence of vegetation. We simulated vegetation following a picture recently introduced by Nishimori and Tanaka (2001), and we could perform the first computational simulation of this transition.

Furthermore, we have applied our dune model to calculate dunes on Mars. We find from our dune model that dune shapes similar to the ones observed on the floor of martian craters could have been achieved by winds of the scarce atmosphere of Mars in the present. And we also found that a property of the martian saltation must be taken into account for correctly predicting the size of dunes on Mars. Another interesting issue we investigated is whether induration of dunes covered by CO_2 frost — in a sim-

ilar way to an experiment carried out by Kerr and Nigra (1952) where dunes have been covered with oil — could be the explanation for unusual dune shapes observed on the martian north polar region. Supported by the results from our dune model, we concluded that, while vegetation transforms barchans into parabolic dunes on Earth, induration due to CO_2 frost could yield dome-shaped, elliptical and straight, linear dunes on Mars.

2 Transformation of barchans into parabolic dunes: Sand mobility competing with vegetation

One particular factor which can have a significant influence on the dune shape is the presence of vegetation on or around the dunes. A recent investigation of aerial photographs covering a time span of 50 years (Tsoar and Blumberg 2002) found that barchans can invert their shape to form parabolic dunes and vice versa when the amount of vegetation changes. Parabolic dunes are U-shaped dunes the arms of which point toward the direction of the prevailing wind. The amount of vegetation varied over that period because of human activities (such as grazing or stabilization) or because of the power of the wind.

The formation of parabolic dunes has been modeled numerically with a lattice model (Nishimori and Tanaka 2001; Baas 2002). Though the authors find intermediate formation of parabolic dunes, this does not constitute the transition between full-sized barchan and parabolic dunes found in McKee and Douglas (1971) and in Tsoar and Blumberg (2002). This effect has not been investigated theoretically before. We propose a model for vegetation growth taking into account sand erosion and deposition and use the saltation model (Sauermann et al. 2001) for simulating the sand transport which determines the evolution of the dunes.

2.1 Vegetation models

2.1.1 Vegetation Growth:

We propose a continuous model for the rate of vegetation growth, following the idea of Nishimori and Tanaka (2001). Vegetation is characterized by its local height h_v. We suppose that vegetation can grow until it reaches a maximum height H_v, and that the growth process has a characteristic time t_g, which may be enhanced or inhibited depending on the climatic conditions.

Moreover, the vegetation growth rate should be a function of the time rate of sand surface change ($\partial h/\partial t$). After any temporal change of the sand surface h, vegetation needs time to adapt to the new conditions. We introduce this phenomenological effect as a delay in the vegetation growth. In this way, the following equation holds:

$$\frac{dh_\mathrm{v}}{dt} = \frac{H_\mathrm{v} - h_\mathrm{v}}{t_\mathrm{g}} - \left|\frac{\partial h}{\partial t}\right|. \tag{6}$$

If the second term on the right-hand side of eq. (6) is larger than the first one, i.e. if the erosion rate is sufficiently high, then dh_v/dt becomes negative, which means that vegetation dies since its roots become exposed (Tsoar and Blumberg 2002).

2.1.2 Shear Stress Partitioning:

The shear stress partitioning is the main dynamical effect of the vegetation on the flow field and, hence, on the sand transport. The vegetation acts as roughness that absorbs part of the momentum transfered to the soil by the wind. Thus, the total surface shear stress is divided into two components, one acting on the vegetation and the other on the sand grains. The fraction of the total shear stress acting on the sand grains can be described by the expression (Buckley 1987)

$$\tau_\mathrm{s} = \tau\left(1 - \frac{\rho_\mathrm{v}}{\rho_\mathrm{c}}\right)^2, \tag{7}$$

where τ is the total surface shear stress, τ_s is the shear stress acting on the non-vegetated ground, ρ_v is the vegetation density, defined as $(h_\mathrm{v}/H_\mathrm{v})^2$, and ρ_c is a critical vegetation density that depends mainly on the geometric properties of the vegetation (Pye and Tsoar 1991).

Equation (7) represents a reduction of the shear stress acting on the sand grains, which also yields a reduction of the sand flux. Both equations (6) and (7) contain the interaction between the vegetation and the sand surface. One implication of eq. (6) is that at those places where sand erosion or deposition is small enough vegetation grows. Afterwards, the consequent decrease of the shear stress (eq. (7)), and also of the sand flux, yields sand deposition, which in turn slows down the growth of vegetation.

2.2 Results

We performed simulations placing a 4.2 m high barchan dune on a rock bed and then allowing the vegetation to grow. A zero influx and a 0.5 m/s upwind shear velocity are set. We also fixed $\rho_\mathrm{c} = 0.5$, a typical value for spreading herbaceous dune plants (Pye and Tsoar 1991) and $H_\mathrm{v} = 1.0$ m. Finally, the dune model parameters are as in Sauermann et al. (2001).

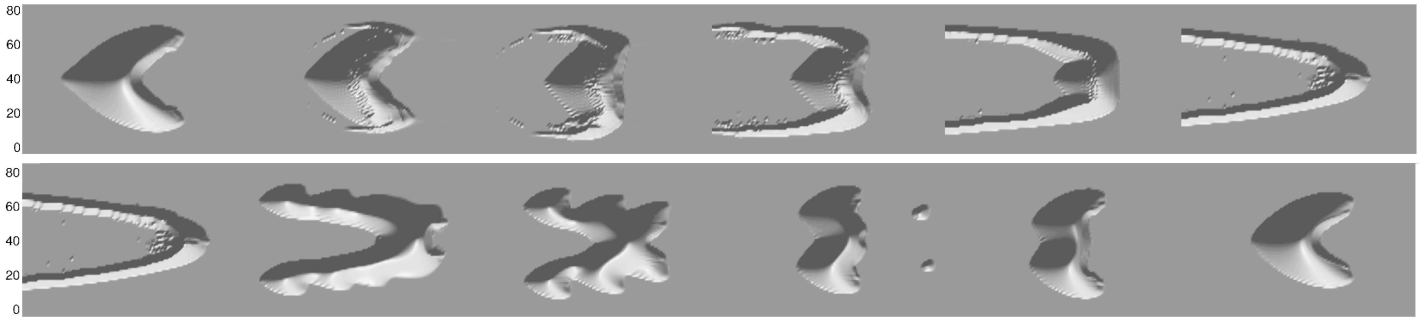

Figure 2. Evolution of an initial barchan dune to a fixed parabolic shape and vice versa. Top: Transformation of barchan into parabolic dune (from the left to the right) with a characteristic time $t_{\rm g} = 7$ days (the evolution of vegetation appears in figure 3). Bottom: After vegetation is removed, the opposite process occurs (from the left to the right) and a barchan shape is achieved.

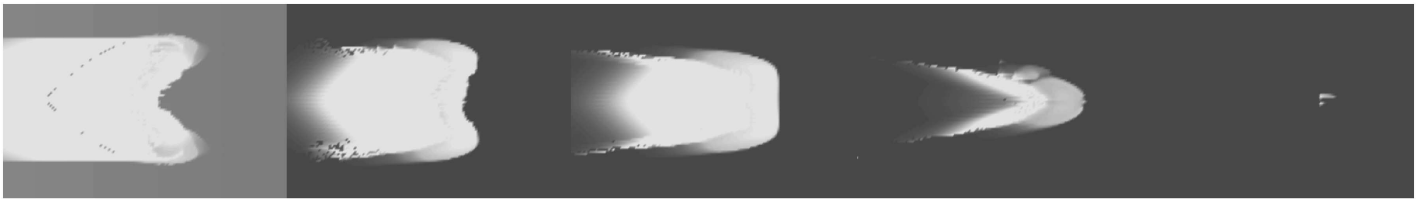

Figure 3. Evolution of the vegetation density in a barchan-parabolic transformation for a vegetation characteristic growth time of 7 days (see upper part of Figure 2). Black means complete covering by vegetation and white means no vegetation.

We studied the influence of the vegetation characteristic growth time $t_{\rm g}$, which contains the information of the growth rate and which, hence, controls the strength of the interaction between the dune and the vegetation.

The upper part of Figure 2 shows snapshots of the evolution of a barchan dune under the influence of vegetation with a characteristic growth time of 7 days. Calculations were performed with open boundaries and a zero influx, which means vegetation is high enough to inhibit sand transport on the flat ground. The evolution of the vegetation density is shown in Figure 3. Initially, the vegetation invades those places where sand erosion or deposition occurs at a small rate, i.e. the horns, the crest and the surroundings of the dune. There, the soil was covered by sand, and, as a consequence of our model, it needs a time $t_{\rm g}$ to recover. As the vegetation grows, it traps the sand, which then cannot reach the lee side. There, the vegetation cover increases. On the other hand, the vegetation on the windward side is eliminated because its roots are exposed as the dune migrates. However, at the horns the vegetation growth is fast enough to survive the low sand deposition and, thus, sand accumulates there. Hence, whereas the central part of the dune moves forward a sand trail is left behind at the horns. This process leads to the stretching of the windward side and the formation of a parabolic dune. This picture is in accordance to a recent conceptual model to explain such transformation based on field observations (Tsoar and Blumberg 2002).

The bottom of figure 2 shows the inverse process. After eliminating all vegetation and setting a constant influx of 0.005 kg/m·s, the parabolic dune is fragmented into small barchanoidal forms which nucleate into a final barchan dune. Although the transformation from parabolic into barchan or transverse dunes have been observed (Anton and Vincent 1986), this fragmentation does not occur in nature because the vegetation is eliminated gradually from the parabolic dune — it leaves the central part of the dune first, but still remains at the lateral trails.

Both the transition from a barchan into a parabolic dune and the parabolic shape obtained strongly depend on the vegetation's growth rate. Figure 4(b), (c) and (d) show the final parabolic dune for three values of $t_{\rm g}$ (see figure caption). As expected, a longer parabolic dune emerges for a smaller vegetation growth rate, i.e. a higher $t_{\rm g}$. On the other hand, if $t_{\rm g}$ is too high, the vegetation cover is not enough to complete the inversion process (Figure 4(a)). In this case the barchan keeps its shape but leaves lateral sand trails covered by plants. However, due to the constant loss of sand at the arms, the barchan decreases in size until it gets finally stabilized by vegetation.

Notice that the parabolic dunes are slightly asymmetric (Figure 4) despite the initial condition being symmetric. This surprising result is the consequence of the interaction of the vegetation with the sand bed. Once vegetation grows, it protects the soil from erosion. This enhances the growth process, which in turn, increments the soil protection and so on. This mechanism amplifies small asymmetries in the vegetation

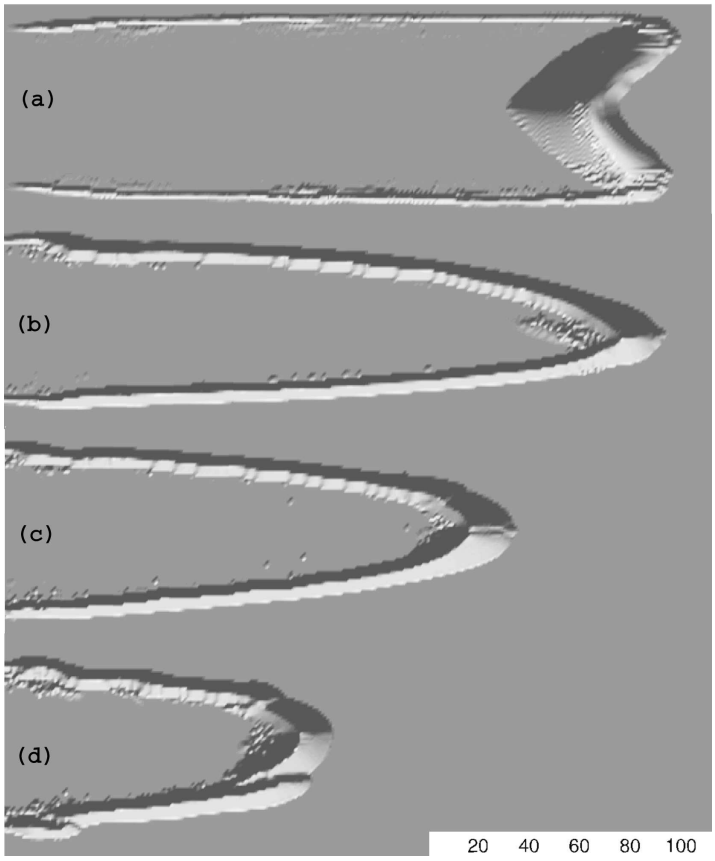

Figure 4. Final or stationary states starting with one barchan dune under the influence of vegetation with different growth rates.The vegetation characteristic growth times are: (a) 12, (b) 8, (c) 7 and (d) 4.6 days. The parabolic dunes are (b) 260 m, (c) 200 m and (d) 130 m long. Note that in (a) the vegetation cover is not dense enough to transform a barchan dune into a parabolic one.

cover. In our simulation, the initial small asymmetries are due to numerical inaccuracies. In nature, they are a consequence of random factors influencing vegetation growth, like, among others, fluctuations in the wind strength and animals.

2.3 Summary

We performed a numerical simulation of the influence of varying amounts of vegetation on dune shapes. We proposed a continuum model describing vegetation growth (eq. (6)). Taking into account the partitioning of the shear stress between the plants and the ground, we used the continuum saltation model to simulate the evolution of the dune shape.

We have reproduced the observed effect of the transition between barchans and parabolic dunes. After a parabolic dune is formed, it is completely covered by vegetation and rendered inactive. So far we could not find any prototype data supporting the time-scales indicated by the model. We have found that the final shape of the parabolic dune evolving from a barchan depends strongly on the growth rate of the vegetation. Slow-growing plants only slow down the arms of the barchan and do not transform it completely into a parabolic dune. The faster the plants grow, the faster the transformation is completed and the shorter are the arms of the resulting parabolic dune.

A quantitative comparison of the results from our vegetation model with data on parabolic dunes measured in the field will be the subject of future work. This will be carried out after our field trip to a parabolic dune field in Northeastern Brazil during the current year.

3 The shape of the barchan dunes in the Arkhangelsky Crater on Mars

3.1 Mars dunes

There are dunes also on the Planet Mars. Sand dunes have been found on Mars for the first time in Mariner 9 images of the Proctor Crater, within the southern highlands of Mars (McCauley et al. 1972; Sagan et al. 1972). Since then, other Missions sent to Mars provided us with thousands of images which revealed a rich diversity of dune shapes including barchans, transverse dunes, and also linear and star dunes (Edgett and Blumberg 1994). With the high resolution images available of Mars, e.g. those from the Mars Global Surveyor (MGS) Mars Orbiter Camera (MOC), the study of the Martian surface has become an issue essentially geologic, rather than a subject of the Space and Planetary Science.

While it appears evident that the martian surface has been steadily modified by aeolian processes, it is difficult to know whether martian dunes are in general active (moving) in the present. Sporadic coverage by orbiting spacecraft could generally not detect dune motion in the past few Martian decades (Williams et al. 2003). This could be a result for instance of currently insufficient wind strength and/or too low rate of dune motion to be measured. In some locations on Mars, it is even plausible that dunes are immobilized or indurated as commented later in Section 4.

But if Mars dunes are in fact inactive today, what about their age? Atmospheric conditions on Mars may have changed dramatically since the origin of the planet. Mars has been gradually losing atmosphere over the last billions of years mainly due to the impacts of meteorites and the low planetary gravity, $g = 3.71\ \mathrm{m/s^2}$, which is almost one third of the earth's gravity, $g = 9.81\ \mathrm{m/s^2}$. While the atmosphere of Mars 4 billions of years ago might have been as dense as the terrestrial atmosphere in the present (Melosh and Vickery 1989), $1.225\ \mathrm{kg/m^3}$, the density of the martian air today is only $0.016\ \mathrm{kg/m^3}$ (CO_2 at temperature of 200 K and pressure of 6.0 mb (MGSR Science Team 2005)). The time at which this density value

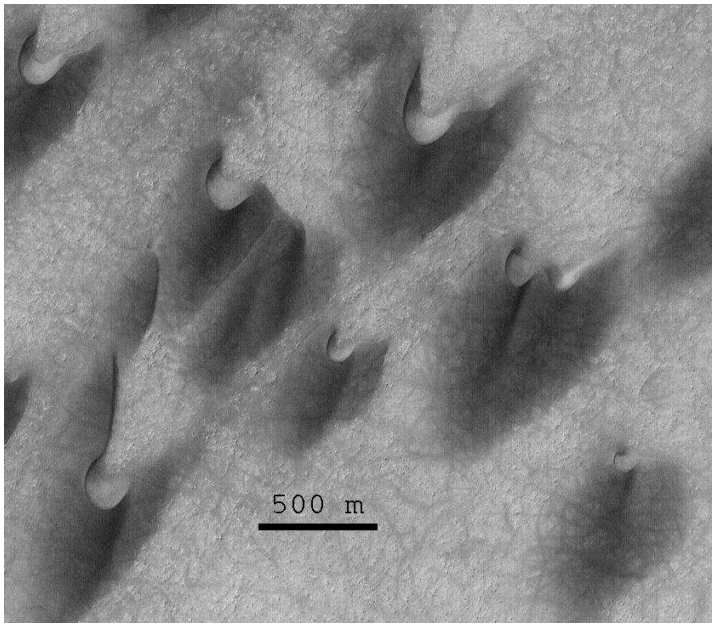

Figure 5. Barchan dunes in the Arkhangelsky Crater, Mars ($41.2°$ S, $25.0°$ W). Image: MGS Mars Orbiter Camera (MOC), 2004.

has been achieved is not known. One motivation to study dunes on Mars with our model is that a study of martian dunes may contribute data on the geological history of the planet, and also help the understanding of aeolian systems and climate conditions of Mars (Bourke et al. 2004a).

Barchan dunes are certainly the most simple and best understood type of dune. Therefore, we started our exploration of Mars dunes with the investigation of a field of barchan dunes located in the Arkhangelsky Crater on Mars ($41.2°$ S, $25.0°$ W), one image of which is shown in fig. 5. Our goal is to use the dune model to reproduce the dune shape observed in fig. 5 using parameters for Mars. We are interested in answering the following question: Has it been possible that these dunes formed under the present atmospheric conditions of Mars? Using the values of martian atmospheric density and gravity, our first aim is to find the conditions of wind and sand flux which define the dune shape observed in fig. 5.

3.2 Model parameters for Mars

Many of the model parameters we need to calculate dunes on Mars are known from the literature. Some of these parameters have been mentioned above — the gravity g and atmospheric density ρ_{fluid}, pressure P and temperature T. Recent Mars Missions obtained important data on sand and wind conditions on Mars, as detailed below, which we use in our calculations.

3.2.1 The sand of Mars dunes

Martian barchans display some essential differences in relation to their terrestrial counterparts. Thermal inertia studies, for example, have shown that the sand of martian dunes is coarser, with a mean grain diameter $d = 500 \pm 100\mu$m (Edgett and Christensen 1991), while the size distribution of sand grains of most terrestrial dunes presents a maximum around $d = 250\mu$m (Pye and Tsoar 1991). Furthermore, it is known that dunes on Mars are made of grains of basalt (Fenton et al. 2003), while terrestrial dunes are constituted by quartz grains. The angle of repose θ_{r} of the sand on Mars, or the inclination of the dune slip face has been found to be close to the terrestrial value, $\theta_{\text{r}} \approx 34°$ (Greeley and Iversen 1984; Williams et al. 2003).

3.2.2 Threshold wind velocity for saltation

The dynamics of saltating grains on Mars has been extensively studied by many authors, both using numerical calculations and from wind tunnel experiments on martian atmospheric conditions (White et al. 1976; White 1979; Greeley and Iversen 1984). The threshold wind shear velocity on Mars has been predicted for a wide range of grain sizes (Iversen et al. 1976; Greeley et al. 1980; Iversen and White 1982). For grains of $d = 500\mu$m, for example, a value of $u_{*\text{t}}$ around 2.0 m/s is predicted for Mars. This is ten times larger than the terrestrial $u_{*\text{t}} = 0.2$ m/s (Pye and Tsoar 1991). Notwithstanding, wind friction speed values of this order have been reported several times from Mars Missions observations (Moore 1985; Sullivan et al. 2000; Cantor et al. 2001).

3.2.3 One unknown saltation parameter

From the saltation model parameters listed in Section 1, there is one, γ (eq. (4)), whose value for Mars we did not calculate. While Sauermann et al. (2001) have obtained γ for the case Earth from reported measurements of the saturation time of terrestrial saltation, here we proceeded in a different way to estimate the entrainment rate of grains into saltation, γ, on Mars.

3.3 Simulation of the Arkhangelsky Dunes

We performed simulations with open boundaries and a small influx q_{in} at the inlet, with values typically less than 30% of the saturated flux q_{s}. Such low values for $q_{\text{in}}/q_{\text{s}}$ are characteristic of the interdune in terrestrial dune fields developing on bedrock (Fryberger et al. 1984). A small value of $q_{\text{in}}/q_{\text{s}}$ is also reasonable for the Arkhangelsky dunes since sediment access in craters is very commonly restricted (Bourke

et al. 2004a). In this way, we need to find for which values of γ and the shear velocity u_* — which is set of course larger than $u_{*t} = 2.0$ m/s — the model reproduces the dune shape in the Arkhangelsky Crater. The initial surface is a gaussian sand hill (fig. 6) with dimensions of the order of the dune sizes observed in fig. 5.

We proceed in the following manner. First, we set the value of γ for Mars equal to the earth's (Sauermann et al. 2001) and we see if it is possible to find the Arkhangelsky dunes for some value of the wind shear velocity u_*. We obtain the surprising result that no dune appears for any value of u_* in the range of estimated wind friction speeds on the Mars Exploration Rover Meridiani Planum (Sullivan et al. 2005) and Viking 1 (Moore 1985) landing sites on Mars, i.e. for u_* between 2.0 and 4.0 m/s. In other words, the gaussian hill does not develop slip face and disappears because its size is below the critical one for dune formation (fig. 7).

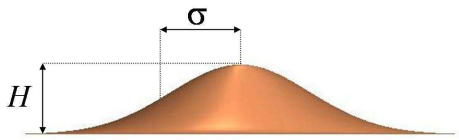

Figure 6. The initial surface is a gaussian hill of height H and characteristic length σ.

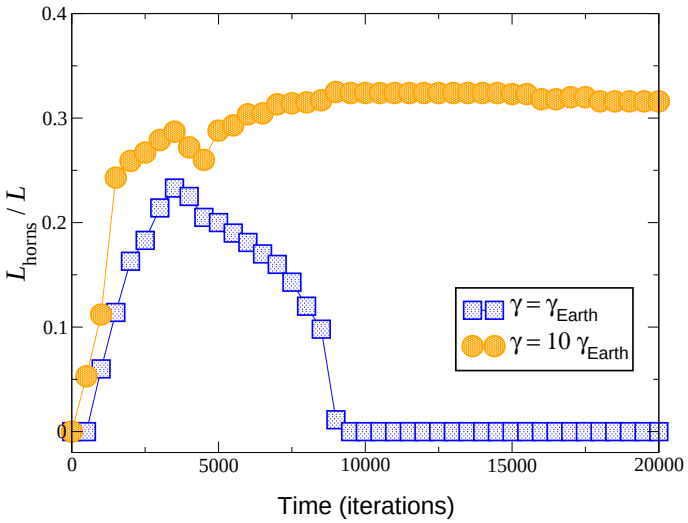

Figure 7. Time evolution of the dune horns length L_{horns} relative to the dune length L using $\gamma = \gamma_{\text{Earth}}$ (squares). In this case, the gaussian in fig. 6 does not achieve an equilibrium barchan shape, and disappears after the sand is blown away, while barchan dunes are obtained with $\gamma = 10\,\gamma_{\text{Earth}}$ (circles). Calculation was performed with $u_*/u_{*t} = 1.75$.

However, if the parameter γ, i.e. the number of grains entrained by the air is of the order of 10 times the earth's then dunes are obtained. Furthermore, as shown in fig. 8, we find that the elongated shape of the Arkhangelsky dunes is in general obtained for a shear velocity close to the threshold. As u_* increases, for a constant value of γ, the dune shape deviates from the Arkhangelsky dunes. One conclusion we get from our calculations, thus, is that the shear velocity in the Arkhangelsky Crater must be close to the threshold friction speed, and probably around 3.0 m/s. Figure 9 shows one dune calculated with this u_* value together with a MOC image of one Arkhangelsky dune.

3.3.1 Interpretations and summary

We remark that our value of u_* is an intermediate value between estimated friction speeds at Pathfinder (Sullivan et al. 2000) and Viking 1 (Moore 1985) lander sites on Mars. On the other hand, why should γ be larger on Mars? As mentioned above, the larger the value of γ, the larger the number of grains a percentual increase of the wind strength relative to the threshold succeeds in entraining into the saltation layer. On the other hand, the grains which are entrained by the wind come mainly from the splash after grain-bed collisions. Therefore, we interpret the larger value of γ on Mars as a result of the larger amount of splashed grains, which may be understood as a consequence of the larger velocity reached by saltating grains on Mars.

The mean velocity of the saltating grains calculated with the dune model is around 16.0 m/s, while for Earth the grain velocity is approximately 1.6 m/s. It follows that the momentum transferred by the impacting grains to the sand bed is much larger on Mars than on Earth, what is associated with much larger splashes after impact on Mars. This picture is in agreement with the observation that the number of ejecta after splash is proportional to the velocity of the impacting grain (Anderson and Haff 1988). In fact, it has already been observed that, while on Earth a single grain-bed collision results in ejection of only a few grains, on Mars the number of splashed grains may be of the order of one hundred (Marshall et al. 1998).

What is the consequence of a larger entrainment rate of grains on Mars? A faster population increase of saltating particles amplifies the "feedback effect", which is the decceleration of the wind due to the momentum transfer of the air to the grains (Owen 1964). Consequently, a larger splash has an astonishingly important implication for the macroscopic scale of sand patterns: it reduces the distance after which the maximum amount of sand which can be transported by the wind is reached, and the minimum size below which sand hills are continuously eroded and disappear.

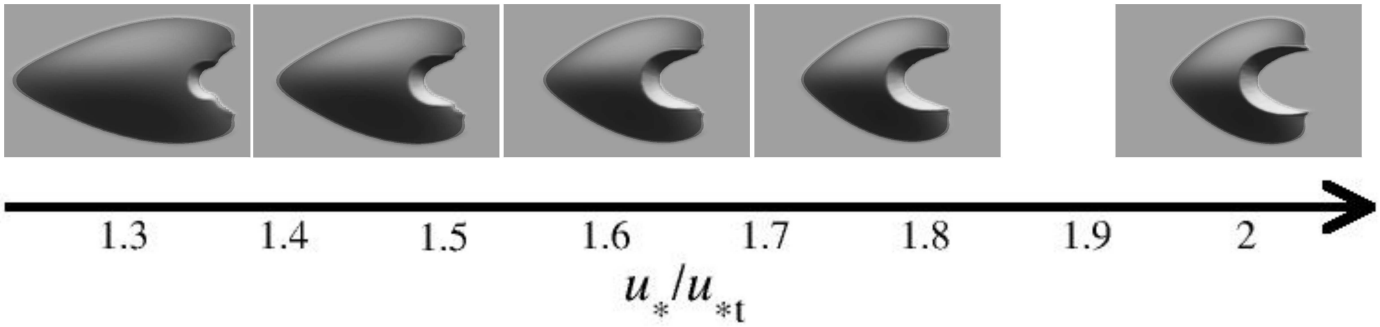

Figure 8. Barchan dunes of width $W = 650$ m calculated using parameters for Mars, with $\gamma = 10\,\gamma_{\rm Earth}$, and different values of wind shear velocity u_* relative to the threshold u_{*t}. We find $u_*/u_{*t} \approx 1.45$ or u_* around 3.0 m/s in the Arkhangelsky Crater.

In the model the information of the splash is incorporated in the parameter γ. We notice that an increase in the value of γ means a decrease in the saturation length of the flux (eq. (3)), as expected — the more grains the wind succeeds entraining saltation, the faster the flux should saturate. Since the saturation length is the relevant length scale of barchan dunes, our calculations reveal that this property of the martian splash must be taken into account for correctly predicting the size of dunes on Mars. We have recently found that if the larger splash on Mars is accounted for in the calculations, we can reproduce not only the dune shape as reported here but also the minimal dune size and the dependence of the dune shape on the size (Parteli et al. 2006). The characteristic length of flux saturation is given by the saturation length $\ell_{\rm s}$ (eq. (3)), and the distance after which the flux saturates is in fact around 7 times $\ell_{\rm s}$. While the saturation length $\ell_{\rm s}$ on Earth is around 50 cm — which is calculated from eq. (3) with $u_* \approx 0.37$ m/s obtained from measurements and calculations of wind friction speed in northeastern Brazil (Jimenez et al. 1999; Sauermann et al. 2003; Parteli et al. 2006) — we have obtained $\ell_{\rm s} \approx 17$ m for Mars using the parameters mentioned above, with which we reproduced the Arkhangelsky dunes. The minimal dune width obtained from simulations is around 10 times $\ell_{\rm s}$, both using parameters for Mars and for Earth (Parteli et al. 2006). Indeed, if the value of γ on Mars were the same as on Earth, the saturation length and therefore the minimal dune scale on Mars would be 10 times larger. It would be interesting to use this new insight to perform a full microscopic simulation for the saltation mechanism of Mars similar to the one that was recently achieved by Almeida et al. (2006).

The wide range of barchan forms observed on Mars is a consequence of the different local physical conditions which dictate sand transport (Bourke et al. 2004a). We are presently carrying out a study of the dune shape as a function of the sand flux under different atmospheric and wind conditions valid for Mars. In Section 4 we present another mechanism that appears to be relevant to explain exotic dune forms on the Martian north polar region.

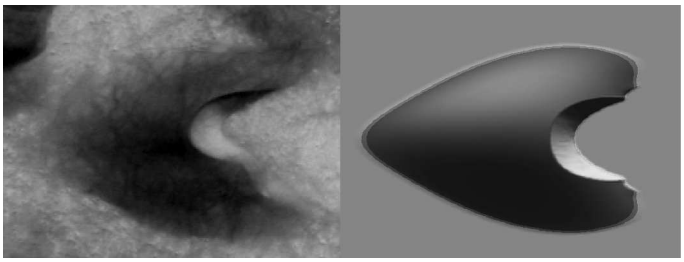

Figure 9. MOC image (left) and calculation (right) of barchan dune of width 650 m in the Arkhangelsky Crater on Mars. Calculation was performed with $u_* = 3.0$ m/s and $\gamma = 10\,\gamma_{\rm Earth}$.

4 Evidence for indurated sand dunes in the Martian north polar region

The morphology and proximity of differing morphologies of a suite of eolian dunes in the Martian north polar region defy traditional explanation. Unusual features occur in a dune field in Chasma Boreale, in the Martian north polar region. Figure 10 shows examples of the dunes, as seen by the Mars Global Surveyor (MGS) Mars Orbiter Camera (MOC). In this dune field, linear and barchan dunes occur together, side-by-side and in some cases are merged to create a single bedform. The linear dunes lack the sinuosity commonly associated with terrestrial seif dunes (Tsoar 1989) — in other words, these linear features are straighter than their counterparts on Earth. Furthermore, the dunes present an additional puzzle — the barchans are elongated into elliptical forms, and the slip faces are typically small or nonexistent (Figure 11).

4.1 Dune movement and induration

While Martian dunes generally appear to be fresh and have no superimposed impact craters (Marchenko and

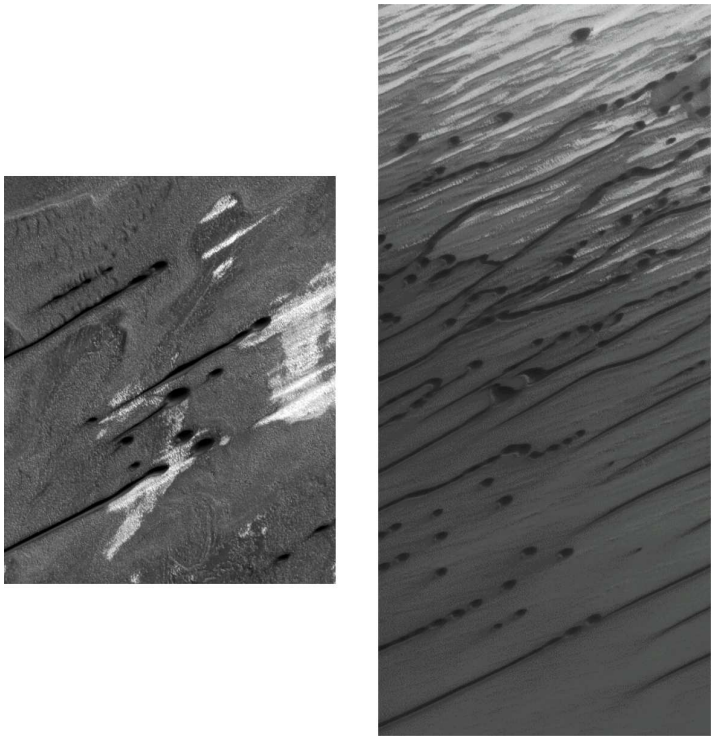

Figure 10. Sub-frames of MGS MOC images showing examples of the elongated, rounded barchans and linear dunes in Chasma Boreale. Both images cover areas about 3 km wide. The picture on the left is from image E01-00104, located near 83.9° N 40.5° W. The right image is from MOC image S02-00901, and is located near 84.2° N 37.9° W. In both cases, sand transport has been from the upper right toward the lower left.

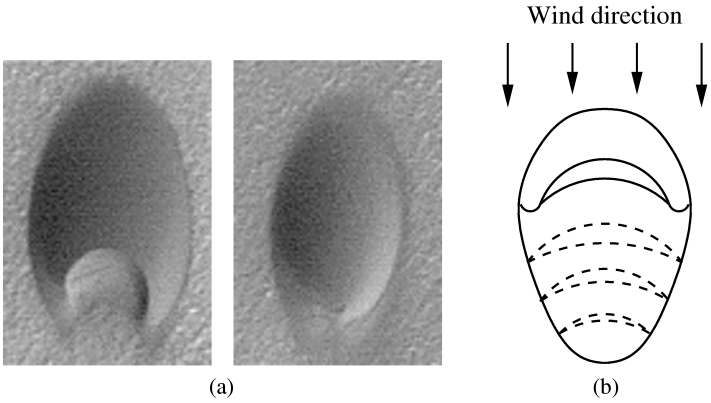

Figure 11. (a) MGS MOC images of a rounded barchan and a dome dune located near 84.9° N 26.6° W, in image M02-00783. The shown parts of the image are each approximately 240 meters wide. (b) Sketch of the deposition in the lee of an oil-soaked barchan (after Kerr and Nigra (1952)). The initial barchan and the final shape are drawn; the dashed lines show the positions of the slip face in intermediate stages, until an elliptical, dome-like shape is produced.

Pronin 1995) — the presence of which would imply antiquity — repeated imaging by MOC has shown no clear evidence for translation of eolian dunes across the Martian surface. The dunes in the Chasma Boreale region were not imaged by Mariner 9 or Viking

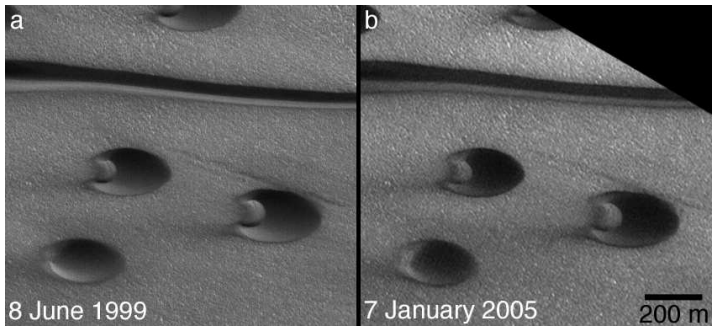

Figure 12. The rounded barchans of Chasma Boreale have been imaged repeatedly by the MGS MOC during the past several Martian years. Relative to features on the substrate across which they are moving, the dunes do not appear to have moved during the mission. The interval between acquisition of the two images shown here is 2.97 Mars years. These dunes include the two shown in Figure 11. (a) Sub-frame of MOC image M02-00783. (b) Sub-frame of MOC image S02-00302. The dunes are illuminated by sunlight from the lower left and are located near 84.9° N, 26.6° W.

at a spatial resolution adequate to see them and measure their movement by comparison with MOC images. Some of the dunes have, however, been repeatedly imaged by MOC during the past four Martian years, and, again, show no evidence for movement (Figure 12). The Chasma Boreale dunes also do not exhibit grooves or steep-walled avalanche chutes. But, the rounded barchans do resemble the oil-soaked dunes of Kerr and Nigra (1952), and the linear dunes simply should not occur with the barchans, unless they are unlike terrestrial linear dunes, and formed—somehow—in a unidirectional wind regime.

We investigate whether it is plausible that the rounded, elliptical dunes in Chasma Boreale could be the product of a process similar to that which was created by successive soaking of dunes in Saudi Arabia with crude oil, and whether the explanation might somehow extend to the occurrence of linear forms in the same dune field. Rather than anthropogenic processes halting dune movement in successive stages, as in the Kerr and Nigra (1952) example, we examine whether induration of dune sand may lead to production of dune forms in Chasma Boreale.

4.1.1 Rounded barchans

Elongated, elliptical, or dome-shaped dunes such as those in Figures 10 and 11, might be the product of successive induration as the slip face advances forward and becomes smaller and smaller, until it disappears, as was observed by Kerr and Nigra (1952) for oil-soaked barchans on Earth. In the Saudi Arabia case, the dunes were sprayed with oil, then additional sand arrived at the fixed dune, blew over its top, and became deposited on the lee side, whereupon the

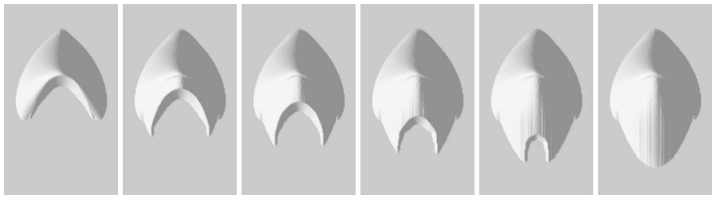

Figure 13. The successive stages of evolution of deposition in the lee of an indurated barchan on Mars. The length of the shown region is 400 meters, the width 240 meters. The first picture shows the initial barchan.

dune was again sprayed with oil. This process continued and, over time, the slip face of each dune became successively smaller, and the dune more rounded and elliptical. This is not typical behavior for lee-side deposition of sand in a dune field, but is a product of the process of successively inhibiting sand movement — in this case, using oil — on the main body of each dune.

The similarity of the oil-soaked dunes to the rounded forms on Mars suggests that the Martian examples could have formed in a similar way, with ice, frozen carbon dioxide, or mineral salts taking the place of oil as the cause for induration. To test the hypothesis under conditions suitable for Mars, we simulated the process of forming a successively-indurated barchan using the appropriate parameters for Mars (Schatz et al. 2006). Figure 13 shows the successive stages of deposition in the lee of the fixed barchan. The shape of the initial dune and the latter successions were all simulated with the same atmospheric conditions, particle properties, and wind speed; the only change was to simulate induration (non mobility) of each successive stage of the dune development, while at the same time adding new sand from the upwind direction.

Some small differences between the simulation in Figure 13 and the satellite image (Fig. 11a) have to be discussed. In the simulations, the brink of the initial barchan is still visible at later stages. In reality, this visible ridge would be slowly eroded even if the dune was indurated. The second discrepancy is that the slip face in the photo appears to be very long, but the foot of the slip face is hard to discern, and a slip face extending nearly to the end of the horns would imply a very high slip face brink, which would be in contrast with the flat rounded shape suggested by the shadows and with the height of other Martian dunes described by Bourke et al. (2004b). The aspect ratio (height divided by length) of our simulated dunes is consistent with the results of Bourke et al. (2004b).

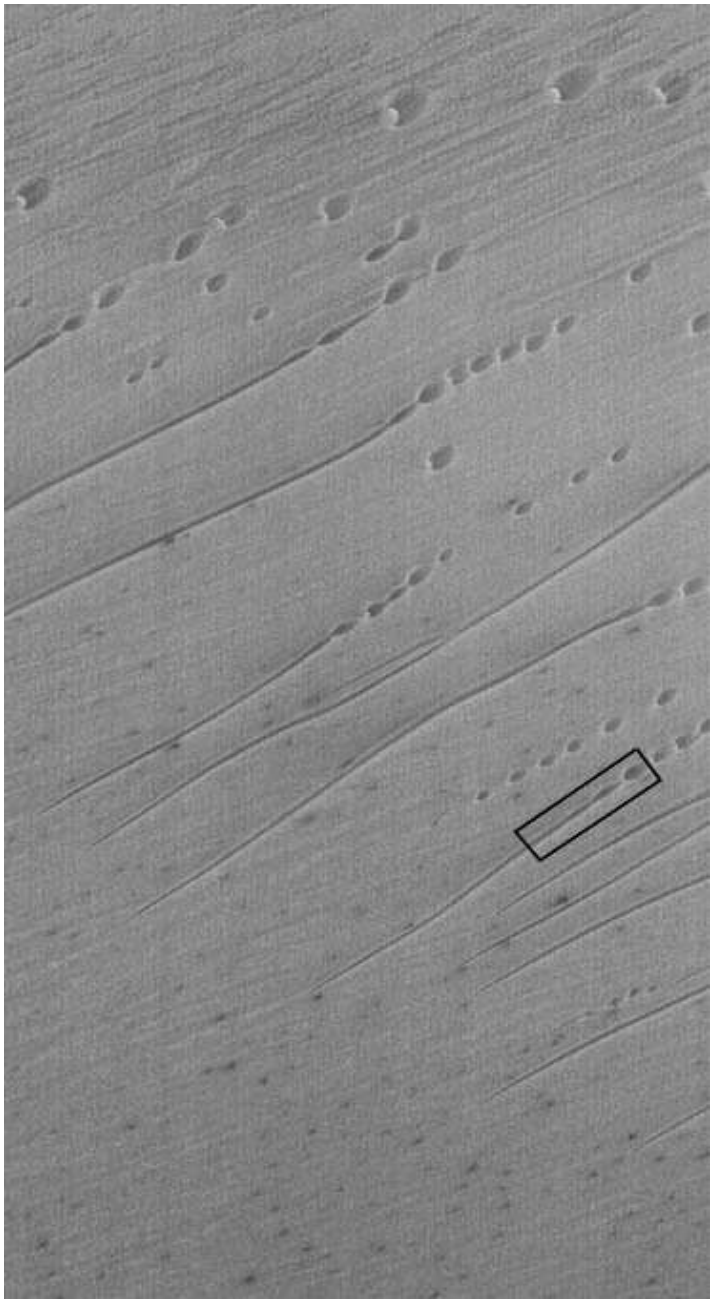

Figure 14. A field of linear dunes in Chasma Boreale. This is a part of MOC image E15-00784, located at 84.24° N 39.95° W. It covers an area about 3 km across. The bright outlines of the dunes and of the ridges in the surrounding region indicate that they are covered by seasonal frost, most likely frozen carbon dioxide. The black rectangle indicates the region selected for our linear dune simulation (see Figure 15).

4.1.2 Chasma Boreale Linear dunes

In addition to the dome-shaped barchans, the region near the Martian north pole exhibits linear dunes that are very straight, unlike their meandering counterparts on earth (Tsoar 1982; Tsoar 1983; Tsoar 1989). These linear dunes occur with the domes and rounded barchans, suggesting that they form in winds flowing parallel to the linear dunes—yet terrestrial experience

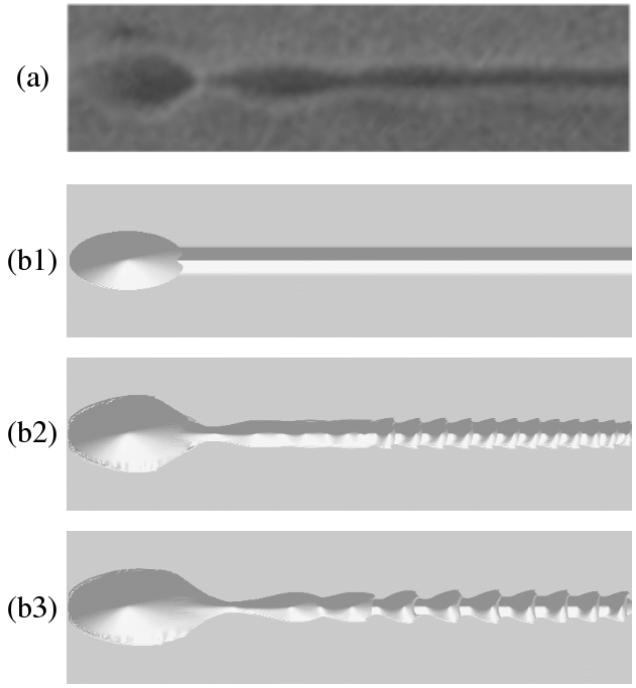

Figure 15. (a) A detail of Figure 14. (b) Simulation of the evolution of a straight linear dune downwind of a dome. Besides small variations in thickness, small barchans can be seen to develop, which are not observed on Mars. From this we conclude that the linear dunes in Figure 14 are indurated.

requires two oblique winds, not a single, unidirectional wind, to create such bedforms.

MGS MOC narrow angle images show that the upwind end of the linear dunes, immediately downwind of the domes, shows a knotted structure (e.g., Figure 14). We have performed a computer simulation of such dunes, starting from a straight ridge in wind direction located just downwind of an unerodable dome. As can be seen in Figure 15, the knots at the upwind end are reproduced in early steps of the simulation. Their formation is analogous to the instability of a sand bed under unidirectional winds (e.g., Andreotti et al. (2002), Schwämmle and Herrmann (2004)). Later on, however, the simulated linear dune decays into a string of barchans. That this does not happen in Chasma Boreale can be explained if the linear dunes are indurated or were formed by erosion in the first place. Although our simulations do not show how the linear forms were initiated, they do suggest— as in the case of the elongated, dome-shaped barchans — that the sands are presently or very recently indurated.

4.2 Summary

The results of our dune model support, in addition to the observations of artificially indurated dunes by Kerr and Nigra (1952), the hypothesis regarding induration of dunes in Chasma Boreale. While basic, typical dune morphologies are a product of wind regime — with, on Earth, contributions from vegetation and moisture — we conclude that induration may be an additional factor that influences morphology of dunes on the Martian north polar region. In the case of Chasma Boreale, induration has led to creation of elongated, elliptical, dome-shaped dunes; elongated barchans with proportionally tiny slip faces; and straight (as opposed to sinuous, like seif dunes) linear dunes that co-exist with barchan forms in a unidirectional, rather than bidirectional, wind regime.

5 Conclusions

In this work, we have presented extensions of the dune model originally introduced by Sauermann et al. (2001) and later improved by Schwämmle and Herrmann (2005) to study dunes with vegetation, and we tested the model to calculate dunes on Mars. We could simulate the transformation of barchans into parabolic dunes, as observed by Tsoar and Blumberg (2002), where we proposed a continuous model for the rate of vegetation growth, following the idea of Nishimori and Tanaka (2001).

Furthermore, we have applied our dune model to calculate the shape of the barchan dunes in the Arkhangelsky crater on Mars. We found that martian dunes may have been formed by winds close to the threshold, under the present atmospheric conditions of Mars, and our calculations reveal that larger splashes on Mars are relevant to explain the size of martian dunes. Finally, application of our model to study north polar dunes on Mars support the hypothesis that the unusual dune shapes observed in the Chasma Boreale region are a result of induration.

Our results are of extreme relevance to understand the formation and evolution of sand dunes in coastal areas, where vegetation very often appears to compete against saltation transport and dune mobility. Furthermore, from calculations of Mars barchan dunes, we gained important insight about the role of the saturation length for the selection of dune size and shape, which is crucial to explain the natural appearence of dunes from the beach. A complete modelling of the formation of coastal dune fields using the results of the present work will be subject of future research.

ACKNOWLEDGMENTS

This work was supported in part by Volkswagenstiftung and the Max-Planck Prize. We acknowledge H. Tsoar and K. Edgett for discussions and J. Harting for a critical reading of this manuscript. E. J. R. Parteli acknowledges support from CAPES - Brasília, Brazil.

REFERENCES

Almeida, M. P., Andrade Jr., J. S., and Herrmann, H. J. (2006). Aeolian transport layer. *Physical Review Letters 96*, 018001.

Anderson, R. S., and Haff, P. K. (1988). Simulation of aeolian saltation. *Science 241*, 820-823.

Anderson, R. S., and Haff, P. K. (1991). Wind modification and bed response during saltation in air. *Acta Mechanica (Suppl.) 1*, 21-51.

Andreotti, B., Claudin, P., and Douady, S. (2002). Selection of dune shapes and velocities. Part 1: Dynamics of sand, wind and barchans. *The European Physical Journal B 28*, 321-329.

Anton, D. and Vincent, P. (1986). Parabolic dunes of the Jafurah desert, eastern province, Saudi Arabia. *Journal of Arid Environments* 11: 187–198.

Baas, A. C. W. (2002). Chaos, fractals and self-organization in coastal geomorphology: Simulating dune landscapes in vegetated environments. *Geomorphology* 48: 309–328.

Bagnold, R. A. (1941). The physics of sand dunes. Methuen, London.

Besler, H. (1997). Eine Wanderdüne als Soliton? *Physikalische Blätter 53(10)*, 983-985 (in German).

Bourke, M. C., Balme, M., and Zimbelman, J. (2004a). A Comparative Analysis of Barchan Dunes in the Intra-Crater Dune Fields and The North Polar Sand Sea. *LPSC XXXV*, 1453.

Bourke, M., Balme, M., Beyer, R. A., Williams, K. K. and Zimbelman, J. (2004b). How high is that dune? a comparison of methods used to constrain the morphometry of aeolian bedforms on Mars. *LPSC XXXV*, 1713.

Buckley, R. (1987). The effect of sparse vegetation on the transport of dune sand by wind. *Nature* 325: 426-428.

Cantor, B. A., James, P. B., Caplinger, M. and Wolff, M. J. (2001) Martian dust storms: 1999 Mars Orbiter Camera observations. *Journal of Geophysical Research 106*(E10), 23,653 - 23,687.

Dong, Z., Huang, N., Liu, X. (2005). Simulation of the probability of midair interparticle collisions in an aeolian saltating cloud. *J. Geophys. Res. 110*, D24113, doi:10.1029/2005JD006070.

Durán, O., Schwämmle, V. and Herrmann, H. J. (2005). Breeding and solitary wave behaviour of dunes. *Physical Review E 72*, 021308.

Edgett, K. S., and Blumberg, Dan. G. (1994). Star and linear dunes on Mars. *Icarus 112*(2), 448-464.

Edgett, K. S., and Christensen, P. R. (1991). The Particle Size of Martian Aeolian Dunes. *Journal of Geophysical Research 96 (E5)*, 22765-22776.

Fenton, L. K, Bandfield, J. L., and Ward, A. W. (2003). Aeolian processes in Proctor Crater on Mars: Sedimentary history as analysed from multiple data sets. *Journal of Geophysical Research 108 (E12)*, 5129. doi:10.1029/2002JE002015.

Foucaut, J.-M., and Stanilas, M. (1997). Experimental study of saltating particle trajectories. *Experiments in Fluids 22*, 321-326.

Fryberger, S. G., Al-Sari, A. M., Clisham, T. J., Rizvi, S. A. R, and Al-Hinai, K. G. (1984). Wind sedimentation in the Jafurah sand sea, Saudi Arabia. *Sedimentology 31*, 413-431.

Greeley, R., Leach, R., White, B., Iversen, J., and Pollack, J. (1980). Threshold windspeeds for sand on Mars: Wind Tunnel Simulations. *Geophysical Research Letters 7(2)*, 121-124.

Greeley, R., and Iversen, J. (1984) Wind as a Geological Process. Cambridge Univ. Press, New York.

Iversen, J. D., Pollack, J. B., Greeley, R., and White, B. R. (1976). Saltation Threshold on Mars: The Effect of Interparticle Force, Surface Roughness, and Low Atmospheric Density. *Icarus*, 381-393.

Iversen, J. D., and White, B. R. (1982). Saltation threshold on Earth, Mars and Venus. *Sedimentology 29*, 111-119.

Jimenez, J. A., Maia, L. P., Serra, J., and Morais, J. (1999). Aeolian dune migration along the Ceará coast, north-eastern Brazil. *Sedimentology 46*, 689-701.

Kerr, R. C. and Nigra, J. O. (1952). Eolian sand control. *Bull. Am. Assoc. Petrol. Geol.* 36: 1541-1573.

Kroy, K., Sauermann, G., and Herrmann, H. J. (2002). Minimal model for aeolian sand dunes. *Physical Review E 66*, 031302.

Marchenko, A. G., and Pronin, A. A. (1995). Study of relations between small impact craters

and dunes on mars, abstracts of the 22nd russian-american microsymposium on planetology, *Tech. Rep. 63-64*, Vernadsky Institute, Moscow.

Mars Global Surveyor Radio Science Team (2005). http://www-star.stanford.edu/projects/mgs/ ("Late Mars Weather").

Marshall, J., Borucki, J., and Bratton, C. (1998). Aeolian Sand Transport in the Planetary Context: Respective Roles of Aerodynamic and Bed-Dilatancy Thresholds. *LPSC XXIX*, 1131.

McCauley, J. F., Carr, M. H., Cutts, J. A., Hatmann, W. K., Masursky, H., Milton, D. J., Sharp, R. P., and Wilhelms, D. E. (1999). Preliminary Mariner 9 report on the geology of Mars. *Icarus 17*, 289-327.

McEwan, I. K., and Willetts, B. B. (1991). Numerical model of the saltation cloud. *Acta Mechanica (Suppl.) 1*, 53–66.

McKee, E. D. and Douglas, J. R. (1971). Growth and movement of dunes at White Sand National Monument, New Mexico. *United State Geological Survey* 750: 108–114.

Melosh, H. J., and Vickery, A. M. (1989). Impact erosion of the primordial atmosphere of Mars. *Nature 338*, 487-489.

Moore, H. J. (1985). The Martian Dust Storm of Sol 1742. *Journal of Geophysical Research 90*(Supplement): D163-D174.

Nalpanis, P., Hunt, J. C. R., and Barrett, C. F. (1993). Saltating particles over flat beds. *Journal of Fluid Mechanics 251*, 661-685.

Nishimori, H. and Tanaka, H. (2001). A simple model for the formation of vegetated dunes. *Earth Surf. Process. Landforms* 26: 1143 - 1150.

Owen, P. R. (1964). Saltation of uniformed sand grains in air. *Journal of Fluid Mechanics* 20: 225 - 242.

Parteli, E. J. R., Durán, O., and Herrmann, H. J. (2006). Minimal size of a barchan dune. Submitted to Physical Review E.

Pye, K., and Tsoar, H. (1991). Aeolian sand and sand dunes. Unwin Hyman, London.

Rasmussen, K. R., Iversen, J. D., and Rautahemio, P. (1996). Saltation and wind-flow interaction in a variable slope wind tunnel. *Geomorphology 17*, 19–28.

Sagan, C., Veverka, J., Fox, P., Quam, L., Tucker, R., Pollack, J. B., and Smith, B. A. (1972). Variable features on Mars: Preliminary Mariner 9 television results. *Icarus 17*, 346-372.

Sauermann, G., Kroy, K., and Herrmann, H. J. (2001). A continuum saltation model for sand dunes. *Physical Review E 64*, 31305.

Sauermann, G., Andrade Jr., J. S., Maia, L. P., Costa, U. M. S., Araújo, A. D., and Herrmann, H. J. (2003). Wind velocity and sand transport on a barchan dune. *Geomorphology 54*, 245-255.

Schatz, V., Tsoar, H., Edgett, K. S., Parteli, E. J. R., and Herrmann, H. J. (2006). Evidence for indurated sand dunes in the Martian north polar region. *Journal of Geophysical Research*, 111(E4), E04006, doi:10.1029/2005JE002514.

Schwämmle, V., and Herrmann, H. J. (2003). Solitary Wave Behaviour of Dunes. *Nature 426*, 619-620.

Schwämmle, V., and Herrmann, H. J. (2004). Modelling transverse dunes. *Earth Surf. Process. Landforms 29*(6), 769-784.

Schwämmle, V., and Herrmann, H. J. (2005). A model of Barchan dunes including lateral shear stress. *The European Physical Journal E 16*, 57-65.

Sullivan, R., Greeley, R., Kraft, M., Wilson, G., Golombek, M., Herkenhoff, K., Murphy, J., and Smith, P. (2000). Results of the Imager for Mars Pathfinder windsock experiment. *Journal of Geophysical Research 105 (E10)*, 547-562.

Sullivan, R. *et al.* (2005). Aeolian processes at the Mars Exploration Rover Meridiani Planum landing site. *Nature 436*, 58-61.

Tsoar, H. (1982). Internal structure and surface geometry of longitudinal seif dunes. *Journal of Sedimentary Petrology* 52: 823–831.

Tsoar, H. (1983). Dynamic processes acting on a longitudinal (seif) sand dune. *Sedimentology* 30: 567–578.

Tsoar, H. (1989). Linear dunes - forms and formation. *Progress in Physical Geography* 13: 507–528.

Tsoar, H. and Blumberg, D. G. (2002). Formation of parabolic dunes from barchan and transverse dunes along Israel's mediterranean coast. *Earth Surf. Process. Landforms* 27: 1147–1161.

Ungar, J. E., and Haff, P. K. (1987). Steady state saltation in air. *Sedimentology* 34: 289–299.

Weng, W. S., Hunt, J. C. R., Carruthers, D. J., Warren, A., Wiggs, G. F. S., Livingstone, I., Castro, I. (1991). Air flow and sand transport over sand-dunes. *Acta Mechanica (Suppl.) 2*, 1-22.

Williams, K. K., Greeley, R., and Zimbelman, J. R. (2003). Using Overlapping MOC Images to Search for Dune Movement and To Measure Dune Heights. *Lunar and Planetary Science XXXIV*.

White, B. R., Greeley, R., Iversen, J. D., and Pollack, J. B. (1976). Estimated Grain Saltation in a Martian Atmosphere. *Journal of Geophysical Research 81 (32)*, 5643-5650.

White, B. R. (1979). Soil transport by Winds on Mars. *Journal of Geophysical Research 84 (B9)*, 4643-4651.